

PAPER

Jammed microgel growth medium prepared by flash-solidification of agarose for 3D cell culture and 3D bioprinting

To cite this article: M Sreepadmanabh *et al* 2023 *Biomed. Mater.* **18** 045011

View the [article online](#) for updates and enhancements.

You may also like

- [Preparation and characterization of PEM-coated alginate microgels for controlled release of protein](#)
Qinhua Zuo, Jianbo Lu, An Hong *et al.*
- [Glassy states in adsorbing surfactant-microgel soft nanocomposites](#)
Sarah Goujard, Jean-Marc Suau, Arnaud Chaub *et al.*
- [3D T cell motility in jammed microgels](#)
Tapomoy Bhattacharjee and Thomas E Angelini

Biomedical Materials



PAPER

Jammed microgel growth medium prepared by flash-solidification of agarose for 3D cell culture and 3D bioprinting

RECEIVED
11 January 2023

REVISED
13 April 2023

ACCEPTED FOR PUBLICATION
5 May 2023

PUBLISHED
18 May 2023

M Sreepadmanabh¹ , Meenakshi Ganesh^{1,2}, Ramray Bhat^{3,4}  and Tapomoy Bhattacharjee^{1,*} 

¹ National Centre for Biological Sciences, Tata Institute of Fundamental Research, Bangalore 560065, India

² Department of Biological Science, Indian Institute of Science Education and Research, Mohali, Punjab 140306, India

³ Department of Molecular Reproduction, Development, and Genetics, Indian Institute of Science, Bengaluru, Karnataka 560012, India

⁴ Centre for BioSystems Science and Engineering, Indian Institute of Science, Bengaluru, Karnataka 560012, India

* Author to whom any correspondence should be addressed.

E-mail: tapa@ncbs.res.in

Keywords: microgel, bioprinting, 3D cell growth medium, porous medium

Supplementary material for this article is available [online](#)

Abstract

Although cells cultured in three-dimensional (3D) platforms are proven to be beneficial for studying cellular behavior in settings similar to their physiological state, due to the ease, convenience, and accessibility, traditional 2D culturing approaches are widely adopted. Jammed microgels are a promising class of biomaterials extensively suited for 3D cell culture, tissue bioengineering, and 3D bioprinting. However, existing protocols for fabricating such microgels either involve complex synthesis steps, long preparation times, or polyelectrolyte hydrogel formulations that sequester ionic elements from the cell growth media. Hence, there is an unmet need for a broadly biocompatible, high-throughput, and easily accessible manufacturing process. We address these demands by introducing a rapid, high-throughput, and remarkably straightforward method to synthesize jammed microgels composed of flash-solidified agarose granules directly prepared in a culture medium of choice. Our jammed growth media are optically transparent, porous, yield stress materials with tunable stiffness and self-healing properties, which makes them ideal for 3D cell culture as well as 3D bioprinting. The charge-neutral and inert nature of agarose make them suitable for culturing various cell types and species, the specific growth media for which do not alter the chemistry of the manufacturing process. Unlike several existing 3D platforms, these microgels are readily compatible with standard techniques such as absorbance-based growth assays, antibiotic selection, RNA extraction, and live cell encapsulation. In effect, we present a versatile, highly accessible, inexpensive, and easily adoptable biomaterial for 3D cell culture and 3D bioprinting. We envision their widespread application not just in routine laboratory settings but also in designing multicellular tissue mimics and dynamic co-culture models of physiological niches.

1. Introduction

Cells grown as monolayers on conventional two-dimensional (2D) culture plates are significantly different from their *in vivo* counterparts in many different ways [1]. In standard flat plate cultures, not only do they exhibit altered morphologies and dynamics [2–4], their gene expression and signal transduction profiles are dramatically altered [5]. Furthermore, cells *in vivo* are exposed to more complex mechanical cues and chemical fields due to their

three-dimensional (3D) packing and access to systemic circulation [6–15]. These mechanical cues from the microenvironment exert dramatic effects on processes as diverse as transcription, adhesion, migration, and metastasis and thus directly control cell fate specification [16–24]. Thus, a 3D culture system that replicates physiologically relevant conditions is essential for probing cellular functioning and behavior *in vitro* [25]. Mimicking such scenarios requires biomaterials with tunable mechanical, chemical, and surface properties. Although, recent technological

advances have addressed many of these requirements [26–30], achieving ubiquity and convenience using currently available 3D cell culture models still remain challenging.

Enabling the widespread adoption and effective utilization of 3D *in vitro* growth media imposes several demands on the design of such platforms. First, to support cell culturing across different time scales, a 3D medium with time-independent material properties is required. These 3D media should allow cell seeding, spatiotemporal probing, and endpoint retrieval of cells without destroying the structural integrity or altering the bulk properties of the matrix. Further, to match the mechanically diverse microenvironments encountered *in vivo*, 3D growth media with tunable stiffness is desirable. Additionally, visualization of cells deep inside the 3D growth media requires optically transparent substrata which can remain stable under standard culture conditions (typically, 30 °C–37 °C). Finally, such biomaterials should be broadly compatible across different cell types to support multi-tissue/multi-organ co-culture systems.

Jammed microgel systems—with their excellent material properties such as precisely tunable stiffness, optically translucent nature, and unimpeded nutrient transport—fulfill a significant fraction of these demands and have been extensively implemented for 3D cell culture and tissue engineering [31–36]. A significant body of work has effectively employed microgel-based scaffolds and inks for applications as diverse as 3D bioprinting of live cells and tissue implants, 3D cell culture of several cell types, *in vitro* vascularization and tissue repair, as well as *in vivo* wound healing [37–50]. Additionally, such jammed microgel systems have self-healing material properties; they can transition from solid-like behavior to fluid-like behavior under applied shear [51]. This physical property has been effectively leveraged for freeform 3D bioprinting applications, allowing an injection nozzle moving through a jammed microgel system to locally shear the packing and inoculate cells in the inter-microgel space that get trapped in space once the nozzle is removed [51–57]. While these innovations have advanced our capabilities for 3D culture and tissue engineering, a handful of limitations still remain to be addressed. Commercially available polyelectrolyte microgels provide negligible control over the composition and charge density of the microgels whereas in-house fabrication of these microgels requires long preparation times with complex synthesis steps. Such caveats complicate their percolation into mainstream biological research.

Here, we present a versatile, cost-effective, highly accessible, and readily adaptable method for the rapid synthesis of jammed agarose microgels as a 3D biomaterial. The broad biocompatibility of agarose due to its inert and neutral nature makes it an ideal scaffold material. Micron-scale droplets of hot agarose

suspension are flash-solidified directly in cold cell growth media to form agarose granules. Our one-step approach obviates several complexities of current microgel fabrication methods—such as dedicated microfluidic setups, complex organic synthesis, extensive wash steps, and trace levels of contaminants. A jammed packing of these agarose granules acts as a versatile biomaterial that can support bacteria, yeast as well as mammalian cells in 3D. These jammed microgel media are translucent and enable embedded 3D bioprinting inside them due to their yield stress behavior and self-healing property. We demonstrate the suitability of these jammed agarose microgels for 3D *in vitro* culture, live cell imaging, antibiotic selection, 3D bioprinting, predetermined structure assembly and retrieval, as well as collagen-based functionalization. This dynamic range of biological capabilities promises a vast potential for tissue bioengineering and sculpting physiologically accurate replicas of diverse cellular microenvironments. Consequently, we believe this to be a valuable and readily adaptable tool for advancing ongoing research in domains such as mechanotransduction, durotaxis, and host-pathogen interactions, among others.

2. Materials and methods

2.1. Microgel synthesis

Jammed agarose microgels are synthesized using agarose (HiMedia, MB002) as the base material. For a limited set of experiments (SI figure 2), agar from two different sources (Sigma, A1296 and Qualigens, Q21185) is also used to demonstrate the general applicability of our manufacturing method. Briefly, agar/agarose solutions of specified concentrations (w/v %) are prepared in double distilled water by suspending the powder form of agarose/agar in room temperature water, followed by heating the mixture in an autoclave to dissolve the solids. Briefly, one part of the warm (~65 °C) molten agar/agarose solution is rapidly injected at a rate of 1 ml s⁻¹ using a 0.5 inch-long, 26 gauge needle (Dispo Van) into four parts of continuous phase solvent (water, DMEM, RPMI, **Yeast-extract Peptone Dextrose** (YPD), or LB) maintained within an ice-bath (0 °C) with vigorous stirring at 1200 RPM. Injection at such a high flow rate, combined with the mechanical agitation, breaks up the molten agarose into micron-sized droplets, which are instantaneously solidified due to the rapid gelation of agar/agarose at low temperatures within the continuous phase. The resultant mixture is subsequently collected and centrifuged at approximately 7000 Xg to yield two distinct phases—a densely packed microgel fraction that settles at the bottom and an overlying liquid solvent layer. The latter is gently decanted. Microgel fractions obtained in this manner are homogenized by gentle pipette mixing to ensure a smooth, uniform consistency. Images

of pre and post-centrifugation microgel samples are obtained using a Nikon D5600.

Carbomer-based swollen granular hydrogels are prepared by dispersing 0.5% (w/v) Carbopol 980 polymer (Lubrizol, CBP1054A) in LB broth, stirring till complete dissolution, and adjusting the pH to 7 with 10 N NaOH.

2.2. Characterization of jammed microgel media

2.2.1. Rheological properties

Rheological properties of the microgels are characterized using an Anton Parr MCR 302 rheometer. For all measurements, we use a roughened cone plate (CP50-4/S, diameter of 50 mm, cone angle of 3.987° , and cone truncation of $498 \mu\text{m}$). Unless otherwise mentioned, all readings are obtained at room temperature. All our rheological measurements are shear-controlled, wherein we apply a known torque to the sample and record the consequent displacement of the measuring probe.

To evaluate the viscoelastic nature of jammed agarose microgels, we apply a low (1%) amplitude oscillatory shear strain over a range of frequencies while recording the G' (storage (elastic) modulus) and G'' (loss (viscous) modulus). Consequently, for a viscoelastic material, G' indicates the elastic solid-like behavior, while G'' quantifies the viscous fluid-like nature. A G' value greater than the G'' indicates that the material predominantly behaves as a solid, while the alternate case implies a viscous fluid. Obtaining measurements across different frequencies helps interrogate the time-dependency (if any) of the material properties. Hence, the oscillatory frequency sweep tests help us establish the soft solid-like nature of our jammed agarose microgels under low shear regimes, which is also time-independent.

Separately, to understand the temperature-dependent gelation dynamics of agarose, we also apply the aforementioned rheological test under two different conditions. In one case, we maintain a sample of molten agarose (1% w/v) over a temperature gradient ranging from 65°C to 0°C by varying the temperature of the rheometer stage. Here, we record both the G' and G'' for oscillatory shear strain over different frequencies. Since we start off with a viscous solution, we expect the $G'' > G'$. We track these two parameters while ramping down the temperature to 0°C and check for the transition point where the G' first exceeds the G'' . This crossover point represents the temperature at which the molten agarose begins to gel, and thereby transitions to a soft solid. The second case is where we maintain the rheometer's measuring stage at 0°C , load a warm molten solution of 1% w/v agarose, and immediately commence measuring the G' and G'' as described above. This test helps characterize the kinetics of the gelation process. We observe that the experimental

setup time, which is of the order of a few seconds, is sufficient for the agarose to gel. Hence, we do not observe a crossover point where $G' > G''$. Rather, the G' remains higher than the G'' from the first timepoint itself, indicating the rapid, almost instantaneous gelation of agarose upon contact with a cold surface.

Several previously reported jammed microgel systems have been shown to exhibit yield stress behavior. Briefly, these microgels are fluidized upon application of high shear rates while reversibly transitioning to a soft solid-like nature under lower shear. This is an important property for 3D printing. The fluidizable nature is necessary for the printing nozzle to freely translate within the microgel bath, while the solid-like properties are required to stably hold the extruded structures in place. To check for the yield stress nature of our jammed agarose microgels, we apply a unidirectional shear at varying rates (30 s for each) while recording the shear stress response. At higher shearing rates, we observe a linear relation between the applied shear and the recorded stress. However, a plateauing trend for the stress response below a certain shear rate indicates the presence of yield stress behavior. This is termed the crossover shear rate, i.e. the shear below which the material is a soft solid and above which it is fluidized. These observations confirm the yield stress material properties of agarose microgels.

2.2.2. Particle size distributions

To determine microgel particle sizes, a 1:1000 dilution of the microgels is prepared in water. Particles are imaged using a phase contrast microscope (Nikon Eclipse TE300) under 10X magnification. These images detail 2D projections of 3D microparticles. The micrographs are analyzed in ImageJ by manually segmenting the particle outlines and employing built-in functions for measuring the particle area and perimeter. For our present study, two parameters have been quantified. The first is the square root of the area, which is an approximate indicator of the particle size. To understand the variability in particle shape, we also calculate the shape factor—the perimeter divided by the square root of the area.

2.2.3. Pore size distributions

To determine the inter-particle pore spaces, we use 200 nm fluorescent tracer particles and track their thermal diffusion through the inter-particle pore spaces. Since the agarose microparticles are rigid bodies, the tracer particles only traverse the pores. We disperse a dilute solution of these in jammed 1% agarose microgels prepared in LB and track their thermal diffusion-guided trajectory by acquiring images within a time interval of 17 ms using the 40X objective of an inverted laser-scanning confocal microscope (Nikon A1R HD25). Mapping the

center of each particle over time using a peak-finding function, we obtain their MSD (mean square displacement). The underlying assumption is that over short time scales, the particles may freely explore the pore spaces, with their motion being constricted or altered only via contact with the surfaces circumscribing each pore. Consequently, the particle MSDs should increase linearly with time for such unimpeded motions while plateauing upon encountering the pore's boundaries. The square root of these plateau values added to the particle diameter gives the characteristic smallest pore space dimensions explored by the particles, the 1-CDF (cumulative distribution function) of which we report as the overall pore size distribution for the LB-based 1% agarose microgel.

2.3. *In vitro* experiments

Microgels synthesized using a 1% w/v agarose solution are used for all *in vitro* experiments. Since each cell type has a specific culture media composition optimal for its growth, we vary the continuous phase solvent in the manufacturing process as per requirement. Briefly, bacterial cells are cultured in 2% (w/v) LB (Luria-Bertani) broth (Sigma L3022); yeast cells are grown in YPD (Yeast-extract Peptone Dextrose, with 1% w/w yeast extract (Himedia RM027), 2% w/w tryptone (Himedia RM014), and 2% w/w D-glucose (Qualigens G15405)); and mammalian cells are grown in either DMEM (Dulbecco's Modified Eagle Medium (Gibco, 12100-038), with 10% fetal bovine serum (HiMedia RM10432) and 1% Penicillin-Streptomycin) or RPMI (Roswell Park Memorial Institute Medium (HiMedia AT060), with 20% fetal bovine serum and 1% Penicillin-Streptomycin) culture media.

2.3.1. Cell culture

OVCAR-3, MDA-MB-231, hTERT FT 282, MeT-5A, and NIH-3T3, obtained from ATCC and used for mammalian cell culture experiments are maintained as adherent monolayers in tissue-culture-treated plastic plates. We also employ two different variants of the OVCAR-3 cells—one which stably expresses the green fluorescent protein (GFP) and another which expresses the red fluorescent protein (RFP) [58]. For long-term culture experiments, we include a constitutively blue fluorescent protein (BFP)-expressing line of NIH-3T3 cells, which has the BFP tagged to the histone protein H2B, that allows direct marking of the cell's nucleus. For the cell-retrieval experiment, we use NIH-3T3 cells constitutively expressing GFP throughout their cytoplasm. These are cultured using DMEM (for MDMB-231, FT-282, MeT-5A, and NIH-3T3) or RPMI (for OVCAR-3) complete culture media at 37 °C under 5% CO₂. In all cases, cells are harvested when cultures are 70%–80% confluent, and manually seeded into the agarose microgels prepared using DMEM/RPMI

complete culture media as the continuous phase. These samples are housed in 35 mm glass-bottom tissue culture dishes.

To culture yeast in jammed microgel media, we use *S. cerevisiae*, a widely-studied species of yeast that reproduces by budding. We first prepare an overnight liquid culture in 2 ml of YPD using a 20 µl inoculum from frozen glycerol stocks (1:100 dilution). The culture is grown for 20 h at 30 °C while shaking the sample at 220 RPM until it attains the stationary phase. For subsequent live-cell imaging and growth curve experiments, a small volume (20 µl) from the overnight-grown culture is homogeneously mixed with 980 µl of YPD-based jammed agarose microgels (1:50 final dilution).

Additionally, the present work employs three strains of *Escherichia coli*. These are—a motile wild-type strain, a non-motile strain, and a strain carrying a kanamycin resistance-conferring plasmid. All three bacterial strains constitutively express the GFP throughout their cytoplasm. To culture bacteria in jammed agarose microgels, we first grow an overnight liquid culture in 2 ml of LB broth using a 20 µl inoculum from frozen glycerol stocks (1:100 dilution). These cultures are grown for 20 h at 30 °C while shaking at 220 RPM until they attain the stationary phase. For live-cell imaging, tracking, and growth curve assays, 10 µl of the overnight-grown culture is added to 990 µl of LB-based jammed agarose microgels (1:100 final dilution).

2.3.2. Collagen-infused microgels

To manufacture adherent microgels, we fabricate jammed agarose microgels infused with polymerized Type 1 collagen fibrils within the inter-particle pore spaces. For this, we add a solution of acidic rat tail Type 1 collagen monomers (Invitrogen, A1048301) to pre-made jammed microgel growth media and initiate the polymerization process. Since collagen monomers are suspended within the microgel pores, the fibers formed post-polymerization will also be present in these regions. We homogeneously mix 200 µl of 1% RPMI-based agarose microgel, 2.5 µl of 1 N NaOH, and 100 µl of 3 mg ml⁻¹ Collagen Type I. Immediately following this, cells are dispersed within the sample by pipette mixing and incubated overnight at 37 °C, 5% CO₂. The polymerized collagen is visible as fibrous structures within the pore spaces, which we observe using reflectance with confocal microscopy. Rheological characterization of collagen-infused microgels is performed by loading the jammed microgel sample mixed with collagen monomers (after adjusting pH) onto the pre-heated measuring stage of the rheometer, maintained at 37 °C. This mixture is allowed to polymerize for 45 min, following which we perform small-amplitude frequency sweep as described above to assess the viscoelastic properties of these collagen-infused microgels.

2.3.3. Cell viability

To evaluate the viability of various cell types in DMEM/RPMI-based agarose gels, we employ calcein-AM and propidium iodide (PI)-based staining, which mark the viable and dead cells, respectively. We stain adherent culture plates with calcein-AM (ThermoFisher Scientific, C1430) at a $1 \mu\text{g ml}^{-1}$ final concentration by resuspending from a 1 mg ml^{-1} stock in the appropriate culture media. Plates with the staining solution are incubated at 37°C , 5% CO_2 , for 30 min, followed by replacement with fresh media and a recovery period of 1 h at 37°C , 5% CO_2 . Following this, we harvest the cells and resuspend them in DMEM/RPMI-based agarose microgels. This mixture is subdivided into two fractions for time point-specific imagings at $t = 0$ h and $t = 24$ h. Prior to imaging, the cell-laden microgel samples are stained with PI (HiMedia, TC252) by directly adding the dye to achieve a final concentration of $5 \mu\text{g ml}^{-1}$, followed by incubation for 15 min at 37°C , 5% CO_2 . While imaging, identical optical settings are maintained for both $t = 0$ h and $t = 24$ h samples, following which the total number of live and dead cells are manually tallied for each field imaged.

2.3.4. Long-term culturing of mammalian cells

To maintain mammalian cells for extended periods in the jammed agarose microgels, we first prepare a mixture of the cell pellet (obtained by harvesting and centrifuging the cells) with a solution of collagen monomers (final concentration of 1 mg ml^{-1}) using agarose microgel prepared in the respective culture media to make up the volume, as well as pH adjustment using NaOH. This is then injected into a bath of jammed agarose microgel prepared using the appropriate culture media as the continuous phase, housed in a glass-bottom 35 mm dish. These samples are imaged (confocal z-stacks) every alternate day for the time periods indicated in the experimental details using identical optical settings on all days for a given sample. To test viability, we specifically employed cell lines constitutively expressing a fluorescent reporter protein for these experiments since dye-based stainings do not typically retain optimal levels of fluorescence for extended periods.

2.3.5. Setup for live cell imaging

We use an inverted laser-scanning confocal microscope (Nikon A1R HD25) for all image acquisitions. Specimens for imaging are housed in glass bottom 35 mm dishes. To minimize sample loss due to evaporation, these are covered with a thin film of mineral oil (Sigma, M5904), which allows oxygen to diffuse freely. For live-cell imaging, a stage-top incubator is used to maintain the optimal temperature (30°C for both yeast and bacterial cells, 37°C for mammalian cells).

For time-lapse imaging of yeast growth, we focus on individual yeast colonies using a 40 X objective and

acquire images every 10 min. For time-lapse imaging of bacterial growth, we maintain a field of view with several visible bacteria in focus and acquire images every 60 min. Tracking of individual motile bacteria within the inter-particle pore spaces of the microgel is carried out using a 40X objective with 8X optical zoom, with a temporal resolution of 100 ms between successive frames. For mapping the trajectory of these bacteria, we pseudocolor individual bacterium within a field of view and manually track their center over successive time frames using an ImageJ-inbuilt function for particle tracking.

2.3.6. Growth curves

Well-grown stationary phase cultures of yeast and bacteria, obtained as described in section 2.3.1, are used as the inoculums for growth curve assay samples. For yeast, 20 μl of overnight liquid culture is added to 980 μl of sterile microgel; whereas for bacteria, 10 μl of overnight liquid culture is added to 990 μl of sterile microgel (1:50 and 1:100 dilution, respectively). Mixing is carried out carefully to ensure even dispersion while avoiding the formation of bubbles, as these interfere with the absorbance readings. 200 μl of well-mixed samples are added to separate wells of a 96-well plate, once again exercising caution to avoid forming bubbles. To prevent the gels from drying out, considering the minute volumes involved, double distilled water is added to the vacant wells surrounding the sample. Plates prepared in this manner are incubated at 30°C overnight in an automated multi-well plate reader, programmed to acquire absorbance readings for 600 nm at regular intervals (in our case, once every 10 min). These represent the optical density of the sample over time, which corresponds to the total growth and increase in biomass. Antibiotic treatments are carried out by adding kanamycin (HiMedia RM210) to the microgel samples to achieve a final concentration of $50 \mu\text{g ml}^{-1}$.

2.3.7. Serial passaging of bacterial culture

We demonstrate the capability of our jammed microgel platform for multi-passage culturing of bacteria over hundreds of generations. For this, we grow an overnight culture in 2 ml of LB-based jammed agarose microgel media using a 20 μl inoculum from frozen glycerol stocks (1:100 dilution). This is allowed to grow at 30°C for 48 h, following which a 20 μl inoculum from this is used to inoculate 2 ml of fresh LB-based microgel, with this step being iterated every alternate day for ten successive days. We also acquire confocal z-stack images of the 48-hour grown samples using identical optical settings to observe the bacterial growth over this 10 day period.

2.3.8. Encapsulation protocol

To encapsulate bacteria within agarose micro-particles, 2 ml of a well-grown stationary phase culture of GFP-expressing kanamycin-resistant *E. coli* is

added to 50 ml of molten 1% w/v agarose solution prepared in LB broth. We prefer to use antibiotic-resistant *E. coli* as opposed to the wild-type strain for this particular experiment in order to minimize the potential for contamination during the gel synthesis and centrifugation steps. This is mixed well and rapidly to ensure even dispersion before the molten agarose commences gelation. The subsequent protocol is identical to what has been described above to generate jammed agarose microgels, with the continuous phase solvent being LB broth. The resultant microgel particles contain embedded bacteria, as is observed using microscopy.

2.3.9. Cell retrieval from jammed microgels

We viably retrieve cells suspended in jammed agarose microgels. For this, we first ten-fold dilute a sample of GFP-expressing NIH-3T3 cells embedded in DMEM-based agarose microgels using liquid DMEM. This is homogeneously mixed by gentle pipetting, followed by low-speed centrifugation at 500 xg for 2 min. This step sediments the agarose particles, but is insufficient to sediment an appreciable fraction of cells. The supernatant obtained hence contains the cells, which is transferred to an adherent tissue culture-treated 35 mm plastic dish, and placed under standard culture conditions. We allow the cells to settle and adhere for three hours, following which we replenish the dish with fresh media, acquire images, and return the dish to the cell culture incubator. This is again imaged at the 24 h timepoint, by when the cells have properly adhered and exhibit the characteristic spindle-shaped morphology commonly observed for fibroblasts.

2.3.10. RNA extraction, cDNA synthesis, and qRT-PCR

Please refer to the Extended Methods section included in the supplementary information file for a detailed description of the RNA extraction protocols, cDNA synthesis, and qRT-PCR analysis.

For bacterial RNA extraction, the workflow described herein has been broadly based on a previously outlined method [59]. To prepare samples, we first grow overnight cultures of wild-type *E. coli*, as described above in section 2.3.1. A 20 μ l inoculum from this is added to 5 ml of LB-based jammed agarose microgel. These samples are cultured at 30 °C for 20 h with shaking at 220 RPM until they attain the stationary phase, following which these are processed for RNA extraction. The final pellet obtained is resuspended in 100 μ l of cold nuclease-free water and the sample's RNA concentration is determined using the Qubit Broad Range RNA Assay (Invitrogen, Q10210).

To create 3D microtissues, we first bioprint a homogeneous mixture of NIH 3T3 cells (20 μ l cell pellet), collagen type I (10 μ l of a 3 mg ml⁻¹ stock), and 0.1 NaOH (2.5 μ l) inside a jammed agarose

microgel growth medium. We allow the tissue to stabilize for at least 24 h under standard cell culture conditions (37 °C, 5% CO₂). To extract the RNA, the microtissue fragment is then picked up, washed with PBS, and digested with 1 ml of Trizol (RDP Trio Reagent, HiMedia, MB566). Subsequent steps are undertaken as per the manufacturer's instructions. The final pellet obtained is resuspended in 30 μ l of nuclease-free water, the concentration of which is determined using the Qubit Broad Range RNA Assay.

We prepare cDNA using samples of total RNA extracted from 3D microtissue as described above using the Superscript III First Strand (Invitrogen, 18080-051) kit. The resultant solution is directly used as a template for subsequent PCR amplification.

Expression levels are evaluated using gene-specific primers for the PER2 (Period Circadian Regulator 2), BMAL1 (Brain and Muscle Arnt-like Protein-1), and DBP (D-Box Binding PAR BZIP Transcription Factor). From the cDNA prepared as described above, 3 μ l of a diluted stock was added such as to achieve a final concentration of 15 ng per well in a 384-well plate. This serves as the template for the PCR amplification, which was carried out using the iTaq Universal SYBR Green Supermix (BioRad, 1725121), as per the manufacturer's instructions. The reactions were carried out in an AppliedBiosystems ViiA 7 Real-time PCR System, using the in-built QuantStudio Real-time PCR software for defining the run protocol and data generation.

2.4. 3D bioprinting in agarose microgels

We employ the previously well-described technique of embedded bioprinting in a support bath, using live cells as the bioink. To minimize shear stresses on cells, we generate finer-grained microgels of smaller particle sizes for 3D bioprinting by shearing jammed agarose microgels prepared as described above using a tissue homogenizer (Polytron PT2100). This results in microgels with a lower yield stress, that allows for smoother translation of the 3D printing nozzle. This treatment generates a large number of air bubbles which are easily eliminated with a quick centrifugation step (short spin to 5000 xg), followed by pipette mixing to ensure a homogeneously smooth sample.

Printability tests are carried out using jammed agarose microgels prepared using water as the continuous phase, which are either homogenized or non-homogenized. For printing, we prepare a viscous ink consisting of a 50% (w/v) PEG solution in water with a tinge of black paint added for visibility. This is loaded into a 1 ml syringe attached to a 20 gauge needle. Leveraging custom-designed structural supports, the syringe is loaded onto the pump arm of a 3D printer (Newport, Motion Controller, Model XPS-D). We use custom-written MATLAB codes to operate the printer, wherein we vary both the nozzle translation speed (V) and flow rate (Q) to print straight lines across various combinations of

these two parameters in both homogenized and non-homogenized microgels. The resultant structures are imaged using the confocal microscope, followed by image analysis in ImageJ. We characterize the feature size by measuring the line diameters for each of the V–Q combinations in both types of microgels.

For bioprinting with bacteria, overnight cultures grown as described above are harvested by centrifuging at 5000 xg for 5 min to obtain a dense pellet, which is then directly loaded into the setup described above and used as the bioink. For bioprinting with OVCAR-3 cells, we harvest the cells by trypsinization, collect them as a dense pellet, and proceed in a manner identical to what has been described above for bacterial bioink, except that these are manually injected using a pipette into a bacteria-laden microgel. For retrieving 3D printed structures from the bulk gel, 20 gauge needles attached to a 1 ml syringe are used to selectively extract the element of interest without perturbing the surrounding regions. Post-printing, the microgel samples are layered on top with mineral oil to prevent desiccation.

2.5. Statistical analysis

All graphs represent the mean of the data collected, for the appropriate number of samples as mentioned in the accompanying figure caption. Error bars indicate the standard deviation from the mean.

3. Results and discussion

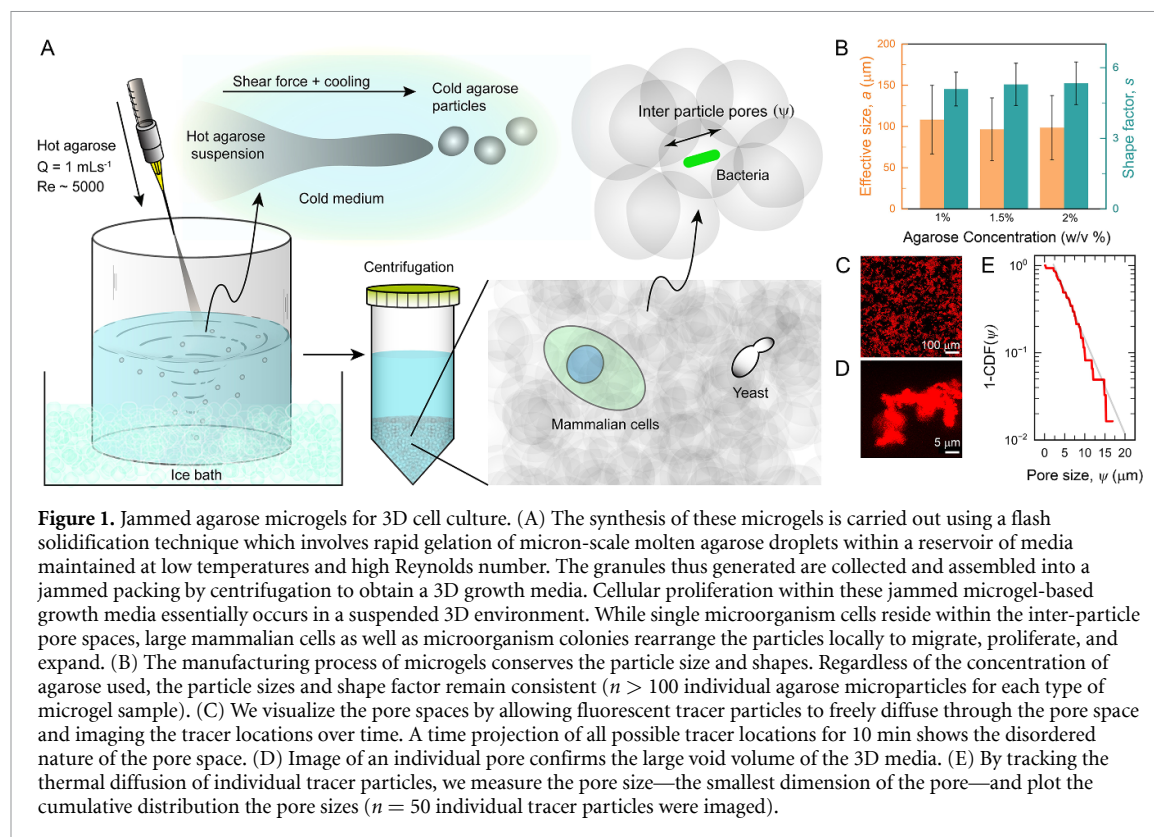
3.1. Synthesis of a neutral jammed microgel system

Several routine laboratory protocols in life science research, such as gel electrophoresis [60], microbial cultures [61], and surface coating [62, 63], employ a variety of chemically inert and porous hydrogel substrates made of crosslinked agarose. The gelation of agarose initiates when its monomeric units, D-galactose and 3,6-anhydrous-L-galactopyranose, crosslink through hydrogen bonding [64]. At high temperatures, disruption of these non-covalent H-bonding produces a viscous agarose solution. At low temperatures (below ~ 35 °C), an aqueous solution of agarose transiently gels to form a solid monolithic matrix. Interestingly, this liquid-to-gel transition of agarose shows thermal hysteresis: while the gelling initiates at ~ 35 °C temperature, the melting of agarose gels starts at a much higher temperature (~ 85 °C) [65]. Thus, after gelation, solid agarose gels remain thermally stable at standard culture temperatures. Furthermore, agarose gels have tunable material properties; the concentration of agarose in these hydrogels regulates their mechanical properties as well as the pore sizes between agarose fibers [66]. Typical pore sizes are much larger (~ 100 nm) than nutrient molecules but smaller than most organisms, which allows for unimpeded nutrient transport while restricting cells to the surface [67]. Hence,

these characteristics, in combination with their neutral and inert nature, render agarose gels highly compatible with several biomedical applications ranging from tissue regeneration for drug delivery and live-cell encapsulation [68].

Drawing our inspiration from the wide application of agarose in biological sciences, in the present study, we introduce a high-throughput flash solidification method to prepare micron-scale granules of agarose hydrogels by leveraging the temperature-dependent gelation process. To quantify the gelation dynamics, a warm solution of agarose (65 °C, 1 wt% solid) is loaded between two parallel plates of a rheometer, on which we perform two different sets of rheological tests. First, we apply a small amplitude (1%) of oscillatory strain at 1 Hz frequency and measure the storage (elastic) modulus (G') and loss (viscous) modulus (G'') as a function of plate temperature. We find that at high-temperatures, G'' is much higher than G' , which is a key property of viscous fluids and indicates that the H-bonding within agarose is yet to initiate. Non-covalent H-bonding interactions increase with the continuous decrease in temperature, thereby increasing the solid-like behavior. Indeed, beyond a crossover temperature (~ 30 °C), G' exceeds G'' when the agarose solution gels into a solid matrix (SI figure 1(A)). Next, we enhance the rate of gelation by dramatically widening the temperature difference between the hot agarose solution and cold surroundings. For these tests, we directly inject the hot agarose solution between two parallel plates of a rheometer maintained at 0 °C and immediately commence the measurements of G' and G'' (SI figure 1(B)). This whole procedure requires less than 10 s: long enough for the instantaneous gelation of the agarose solutions upon contact with the cold surfaces. This rapid liquid-to-solid phase transition is the cornerstone of our microgel synthesis strategy.

More precisely, an autoclaved aqueous suspension of agarose above the gelation temperature (~ 65 °C) is injected via a 26 gauge syringe needle into an ice-cold water bath (0 °C) at a high flow rate of ~ 1 ml s^{-1} . Injection at such a high flow rate produces turbulent flow at Reynolds number ~ 5000 . Simultaneously, the ice-cold water bath is vortexed at 1200 RPM to maintain a turbulent regime. The vigorous and turbulent shear flow breaks up the cold and solidified agarose from the agarose solution and forms micron-scale granules (figure 1(A) and SI figure 2(B)). Maintaining a constant bath to final solid volume fraction, injection at a preferred Reynolds number, precise agarose concentration, controlled vortexing speed, and bath temperature, ensure precise particle sizes. To characterize this, we image individual microgel particles and measure their size. The average particle sizes are very consistent across different batches and are in the order of 100 ± 50 μm (figure 1(B), SI figures 3(A) and (D)). Subsequently, these microgels are randomly packed into a jammed



state via centrifugation, and the supernatant fluid is removed to form a 3D matrix (SI figure 2(A)).

To culture cells in this 3D medium, we need to ensure a smooth transportation of oxygen and nutrients molecules to the cells. In this case, the diffusive transport of nutrients and oxygen is governed by the porosity of the jammed microgel medium. Although the pores inside the individual microgel particles are large enough for nutrient diffusion, there exists another set of inter-microgel pores, which are orders of magnitude larger in size. To quantify the inter microgel pore sizes, we deploy tracer particles and image their motion under thermal diffusion. A time projection (~ 10 min) of all possible positions of the tracer particles indicates the tortuous pore spaces inside the jammed microgel medium (figures 1(C) and (D)). To further characterize the smallest dimensions of these pores, we track the centroid of these tracer particles and measure the cage size from their mean squared displacement (see materials and methods). Similar to many other randomly packed porous media, we find these pore sizes are exponentially distributed (figure 1(E)). By fitting an exponential function to this data, we estimate an average pore size of $4 \mu\text{m}$. Presence of such large pores—which are several orders of magnitude larger than most small molecules—ensures unimpeded supply of nutrients that is critical for the growth and metabolism of cells (figure 1(E)).

Microgel production via flash solidification of agarose solutions overcomes a majority of the

complexities of state-of-the-art microgel manufacturing methods. Current practices of microgel synthesis employ either a bottom-up or top-down approach [69]. In the bottom-up approach, micron-sized crosslinked hydrogel particles are made from a precursor solution either through a precipitation polymerization method—wherein both the monomer and catalytic initiator are soluble, but the insoluble polymeric end product precipitates out—or emulsion polymerization—wherein emulsified droplets of aqueous monomers solutions are polymerized and crosslinked inside an oil bath. However, hydrogel particles produced in these methods require the removal of the solvents and oils through multiple washing and purification steps. In top-down approaches, hydrogels are mechanically sheared into smaller particles, but this requires equipment-specific starting volumes and multiple processing steps. Other drawbacks include long preparation times, low optical transparency, and the presence of tiny fragments of polymer chains that increase the osmotic pressure of the medium. Our approach neatly circumvents these problems by directly injecting hot agarose solutions into an ice-cold liquid culture medium of choice. This ensures we have no unwanted residuals since the only reagents involved are agarose and the growth media itself. Micro-particles thus formed are recovered by centrifugation, yielding a ready-to-deploy jammed microgel system without any downstream processing steps. The supernatant growth medium removed after centrifugation is easily

reusable and hence reduces the wastage of cell growth media in the washing process.

3.2. Characterization of jammed agarose microgels

For long-term cell culturing practices, it is critical for the 3D growth matrix to keep the cells suspended in space—ideally for several days—and allow them to form multi-cellular populations. Although several suspension culture media have been prepared from viscous fluids and utilized to culture cells in 3D, they fail to provide long time stability to individual cells and multicellular structures; suspended cellular populations eventually settle down over time. Thus, a 3D growth medium is preferred to have solid-like behavior. To test if our jammed agarose medium has a solid-like material property, we perform rheological measurements where we apply a small amplitude of oscillatory shear strain (1%) at varying frequencies (1 Hz–0.1 Hz) and measure the shear moduli of the packings. Multiple batches and combinations of jammed agarose media were tested. In all measurements, the storage (elastic) modulus (G') remains frequency independent and higher than the loss (viscous) modulus (G'')—a characteristic behavior of a solid-like material. These measurements confirm that within elastic limits, jammed agarose microgels behave like soft solids with time-independent material properties (figure 2(A), SI figures 3(B) and (E)). Furthermore, a prime motivation for developing 3D culturing systems is to accurately mimic physiological microenvironments with tunable mechanical properties. By regulating the agarose concentration, we control the overall stiffness of the jammed microgels. This tunable stiffness of our microgel system, along with its temporal stability, makes it a reliable scaffold for *in vitro* cell culture.

To accommodate easy placement and retrieval of cells as well as cell proliferation, differentiation, and migration in 3D, the growth matrix should have self-healing material properties and allow for easy remodeling of the cellular microenvironment. For instance, a bacterial colony growing under 3D confinement actively deforms the surrounding matrix and expands over time as individual cells continue to proliferate. Similarly, mammalian cells form spheroids in a 3D culture expands in 3D by actively pushing against its surrounding matrix. We test the self-healing material properties of the jammed agarose microgel media using a rheometer; we apply a unidirectional shear at varying shear rates while recording the stress response for each sample. Similar to previously reported jammed microgel systems [70], we find that the packings of agarose microgels are soft solids that can transition between a fluidized state and a jammed solid state as a function of applied shear. Above a threshold shear rate, they transition from soft solid to liquid-like behavior (figure 2(B), SI figures 3(C) and (F)).

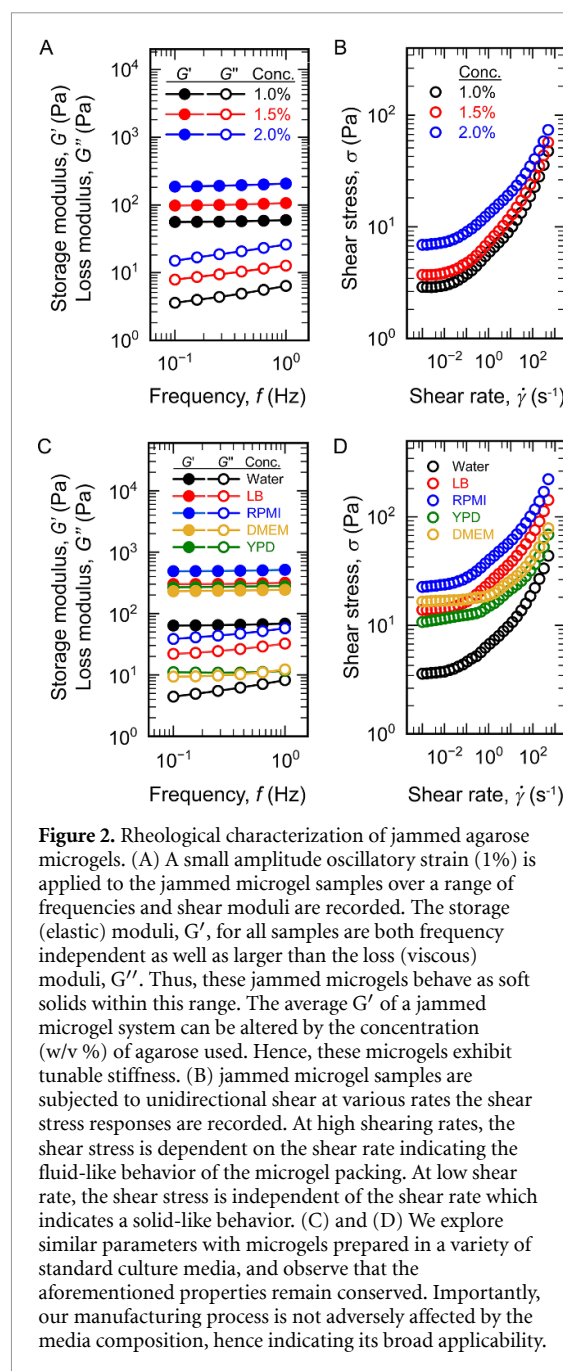


Figure 2. Rheological characterization of jammed agarose microgels. (A) A small amplitude oscillatory strain (1%) is applied to the jammed microgel samples over a range of frequencies and shear moduli are recorded. The storage (elastic) moduli, G' , for all samples are both frequency independent as well as larger than the loss (viscous) moduli, G'' . Thus, these jammed microgels behave as soft solids within this range. The average G' of a jammed microgel system can be altered by the concentration (w/v %) of agarose used. Hence, these microgels exhibit tunable stiffness. (B) jammed microgel samples are subjected to unidirectional shear at various rates the shear stress responses are recorded. At high shearing rates, the shear stress is dependent on the shear rate indicating the fluid-like behavior of the microgel packing. At low shear rate, the shear stress is independent of the shear rate which indicates a solid-like behavior. (C) and (D) We explore similar parameters with microgels prepared in a variety of standard culture media, and observe that the aforementioned properties remain conserved. Importantly, our manufacturing process is not adversely affected by the media composition, hence indicating its broad applicability.

The ability of jammed agarose microgels to transition back and forth between a solid and fluidized state carries significant implications from an experimental perspective. The yield stress property of jammed agarose microgels permits both spatial and temporal micromanipulations without causing plastic deformations or altering the mechanical properties. This flexibility enables sample seeding, retrieval, region/cell-specific probing, as well as the introduction of additional components such as drugs, signaling cues, cellular markers, etc, during the course of an ongoing experiment itself in a user-defined manner. In rigidly cross-linked polymeric scaffolds, it is not possible to extract cells post-seeding, which

precludes possibilities for DNA/RNA/protein extraction or immunostaining without disrupting the bulk structure.

3.3. Jammed agarose microgels for mammalian cell culture

To support and grow cells in 3D, the jammed microgel platform requires a cell type-specific growth medium as the continuous phase between the microgel granules. We accommodate this by synthesizing microgels directly inside standard growth media as the continuous phase and evaluating their material properties. Regardless of the chemical nature of the different growth media, the material properties of jammed agarose microgels remain largely conserved, indicating the broad efficacy of this method (figures 2(C) and (D)). Utilizing the self-healing nature of the jammed microgel media, we directly inject mammalian cells and homogeneously distribute them throughout the 3D media. Furthermore, the jammed microgels prepared with different growth media retain excellent optical transparency (SI figure 4(A)). Leveraging this physical property, we are able to capture high-quality images of living cells expressing a fluorescent reporter (figure 3(A)). Since agarose surfaces do not permit cell adhesion, cells inside the jammed microgels media are held in a 3D suspended state supported by multiple agarose microgel particles (SI figure 4(B)). Additionally, the charge neutrality of agarose eliminates interference with the surface properties and cellular interactions.

However, cellular adhesion to biopolymers is critical for both engineering tissue-like mimics and culturing strictly adherent cell types. To culture adherent cells inside a 3D disordered media, we directly polymerize collagen monomers inside the intermicrogel pores of a jammed agarose microgel growth media to achieve a final collagen concentration of 1 mg ml^{-1} collagen. The collagen monomers polymerize at 37°C , creating a network of fibrils within the pore spaces of the microgel, which alters the pore space geometry by varying the available void space between agarose microparticles. The infusion and polymerization of collagen also changes the rheological properties of the jammed microgels (SI figure 5) which provide further control over the microenvironment stiffness. Cells dispersed through the interparticle pores are able to cluster these fibrils by adhering to them and pulling together several of these, indicating local reorganizations of their 3D microenvironment (figure 3(B)).

Although cellular behavior has been extensively studied inside monolithic biopolymer gels of collagen and laminin-rich basement membrane matrix, the disordered nature of jammed microgels with biopolymers inside the inter microgel pore space helps mimic mechanical regimes and rheological properties broadly similar to that measured in tissues [71]. Our approach allows the study of individual cells in a

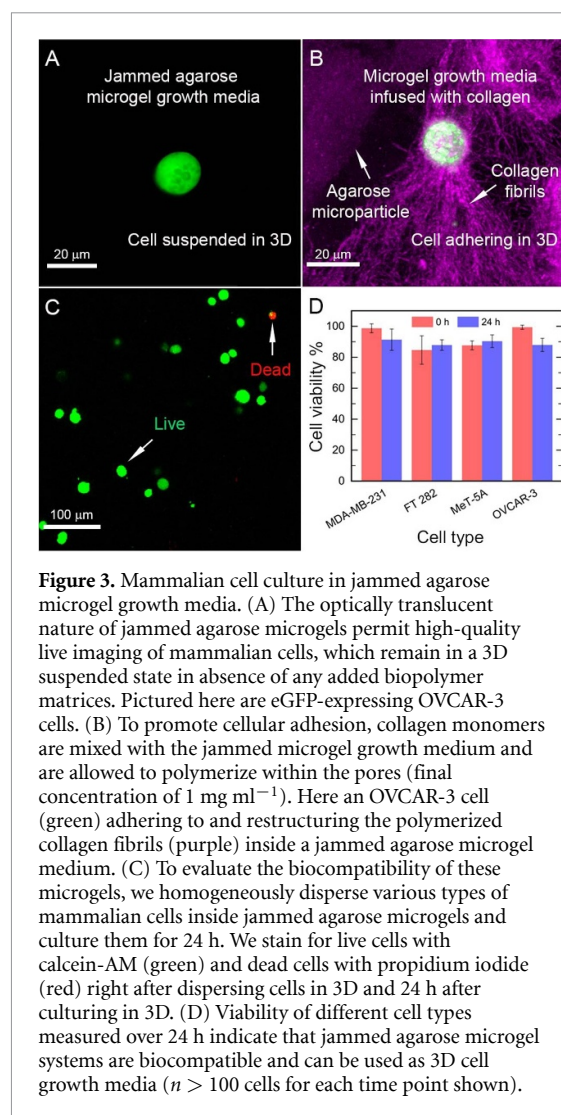


Figure 3. Mammalian cell culture in jammed agarose microgel growth media. (A) The optically translucent nature of jammed agarose microgels permit high-quality live imaging of mammalian cells, which remain in a 3D suspended state in absence of any added biopolymer matrices. Pictured here are eGFP-expressing OVCAR-3 cells. (B) To promote cellular adhesion, collagen monomers are mixed with the jammed microgel growth medium and are allowed to polymerize within the pores (final concentration of 1 mg ml^{-1}). Here an OVCAR-3 cell (green) adhering to and restructuring the polymerized collagen fibrils (purple) inside a jammed agarose microgel medium. (C) To evaluate the biocompatibility of these microgels, we homogeneously disperse various types of mammalian cells inside jammed agarose microgels and culture them for 24 h. We stain for live cells with calcein-AM (green) and dead cells with propidium iodide (red) right after dispersing cells in 3D and 24 h after culturing in 3D. (D) Viability of different cell types measured over 24 h indicate that jammed agarose microgel systems are biocompatible and can be used as 3D cell growth media ($n > 100$ cells for each time point shown).

confined 3D environment in the presence of extracellular matrices. Furthermore, it provides the capability for region-specific manipulation such as introducing chemical cues or sampling a fraction at different time points by leveraging the self-healing properties of the jammed microgels.

A critical goal for 3D culturing setups is to ensure that cells remain viable over sufficiently long durations. We test the biocompatibility of our jammed agarose microgels by assaying for cellular viability over a 24-hour period (figures 3(C) and (D)). Not only are cells stably maintained within these gels, the non-cancerous pleural mesothelial cell line MeT-5A exhibits robust growth and proliferation over this time course. To rule out any cell type-specific effects, we evaluate a panel of different cells, including epithelial ovarian cancer cells (OVCAR-3), hTERT-immortalized fallopian epithelial cells (FT 282), MeT-5A, and the epithelial breast cancer cells (MDA-MB-231). To meet the requirement of cell type-specific culturing media (RPMI for OVCAR-3, DMEM for the others), we simply change the continuous phase during synthesis to generate microgels compatible with each cell type. These results illustrate the broad

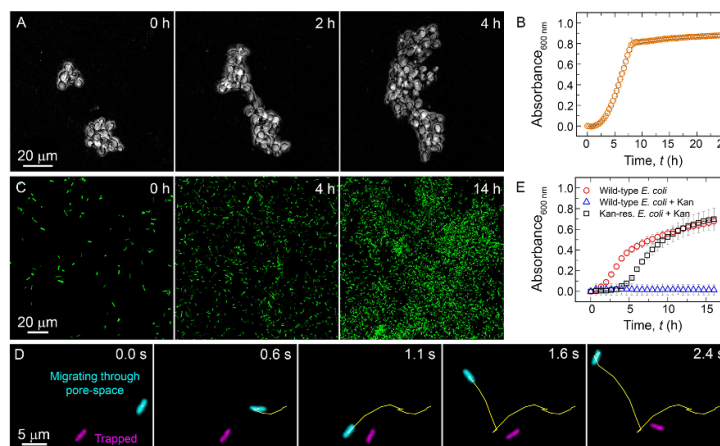


Figure 4. Yeast and prokaryote cell culture in jammed microgel growth media. Our 3D culture media is easily adaptable for a variety of cell types by replacing the continuous phase with a culture media of choice. Here, we show yeast (*S. cerevisiae*) and bacterial (*E. coli*) culture in YPD and LB broth-based jammed agarose microgel. The optically transparent nature of these microgels make them amenable with widely used readout methods such as live-cell imaging—(A) for growing *S. cerevisiae* colonies and (C) for motile GFP-expressing *E. coli*—as well as (B) absorbance-based growth curve assays, as shown for *S. cerevisiae* (shown here, mean and error from three technical replicates). It is also possible to maintain a spatially fixed field of view over several hours with these microgels since they behave as soft solids. This is also enabled by the inert and non-charged nature of agarose, which remains stable at standard culturing conditions, thereby permitting long-term live cell imaging and culturing. Our platform is also suitable for studying the dynamics of motile bacteria, such as the wild-type *E. coli* used here. Within the inter-particle pore spaces, individual *E. coli* bacterium exhibit hopping-and-trapping motion (D), as previously reported in porous granular media. High-resolution tracking of this behavior is enabled by the microgel's optical transparency. The charge neutrality is a critical property of these jammed microgels, which makes them compatible with commonly used charged antibiotics, such as kanamycin. Growth curves in LB-based microgels (E) with and without kanamycin using both wild-type and kanamycin-resistant *E. coli* indicate that this polycationic antibiotic retains its antimicrobial activity in jammed agarose microgels (shown here, mean and error from three technical replicates for each sample type).

applicability of our *in vitro* 3D system for mammalian cell culture. Furthermore, we culture homogeneously dispersed NIH-3T3 cells in jammed microgels for over three weeks (SI figure 6) as well as dense packings of multicellular collectives using two different cell types for at least five days (SI figure 7) without any observed loss in cell viability, which demonstrates the capability of these microgels for long-term culture applications. Similar to what has been shown using PEG hydrogels, the capability to make microgels adherent for cells opens up possibilities to generate micro-patterned gel surfaces with essential growth and differentiation factors interspersed at strategic locales [30, 72–77].

3.4. Jammed agarose microgels for microbial cell culture

To test the suitability of jammed agarose microgels as a versatile biomaterial across different scales, we test the growth and dynamics of yeast and prokaryotes (bacteria) in them. Apart from supporting microorganisms in 3D, jammed microgels also closely mimic their natural habitat. Yeast is widely used to ferment semisolid materials such as dough, whereas bacteria naturally inhabit complex 3D porous environments such as soil, skin pores, gut mucus, and inter-tissue pores. Recently, jammed systems of polyelectrolyte microgels have been utilized for understanding bacterial dynamics within 3D porous media, which has led to a paradigm shift from conventional ideas of motility and spatial interactions

[78–81]. However, the Coulombic interaction of the polyelectrolyte microgels with the components of the dispersed medium poses a critical challenge and limits the possibility of testing the effect of ionic compounds on microbes in porous media. The jammed agarose microgel media—a charge-neutral granular porous 3D matrix—solves this problem.

To culture yeast in agarose microgel media, we homogeneously disperse a commonly used laboratory strain, *S. cerevisiae*, inside the jammed media. The inter-microgel pore space of the 3D media is filled with YPD Medium, which provides a nutrient-rich environment for the yeast cells. Leveraging the optically translucent properties of the agarose microgel medium, we directly visualize the proliferation of yeast colonies using confocal microscopy. This is a consequence of the yield stress nature of jammed microgels—colonies locally and temporarily fluidize the surrounding matrix while growing outward, but they are held in place by the soft solid-like gel (figure 4(A)). To quantify the growth of yeast, we further exploit this optical translucency and use a plate reader to measure the temporal change in absorbance of 600 nm monochromatic light by the overall media. Since, at any time, absorbance is proportional to the total number of cells present, the temporal change in absorbance indicates the growth rate of yeast in the jammed agarose media (figure 4(B)).

Similar to yeast cultures, the jammed agarose microgel media—prepared by infusing LB in the inter-microgel pore space—supports the growth of

bacterial populations. The growth of *E. coli* populations constitutively expressing GFP is directly imaged using a confocal fluorescence microscope (figure 4(C)). However, unlike yeast, *E. coli* cells are motile. While in a homogeneous liquid environment, *E. coli* cells move via run-and-tumble motion, in porous media, the microbial dynamics are governed in large part by the microscale architecture of the system. Recent reports show that these bacteria explore their porous microenvironment by traversing the interconnected pore spaces by hopping—fast-directed motion—between local traps where cellular motion is halted [78, 80, 81]. Similarly, we observe the hopping-and-trapping motility of *E. coli* cells inside the jammed microgel growth media (figure 4(D)) confirming that these cells are proliferating inside a truly disordered 3D media, much similar to their natural habitat. The jammed microgel platform can also be employed for serial passaging of bacterial cultures over several hundreds of generations, which suggests potential applications for understanding the *in vitro* evolution of traits across different mechanical regimes and under 3D confinement (SI figure 8).

While the 3D growth media made from jammed polyelectrolyte microgels have been extensively used to study bacterial colony growth [15], the Coulombic interactions between the microgels and ionic compounds in the media limit their applicability. One such example is antibiotics-based selection—a commonplace practice in microbiology laboratories due to its relative ease of use and efficacy of action. However, several antibiotic molecules are charged species that can be sequestered by the microgels and hence become ineffective. Since a predominant fraction of microbiological research extensively employs antibiotic selection, this presents a considerable barrier to the broader deployment of jammed polyelectrolyte microgel systems. Indeed, inside a 3D medium prepared by jamming negatively charged microgels (carbomer 980), kanamycin—a polycationic aminoglycoside molecule—when used at a concentration of $50 \mu\text{g ml}^{-1}$ —higher than the minimum inhibitory concentration in liquid LB—fails to halt *E. coli* growth (SI figure 9(A)). While kanamycin is rendered ineffective in charged microgels, it restricts the growth of wild-type *E. coli* in neutral jammed agarose microgels (figure 4(E)). This leads to two significant outcomes—one, that charge-neutral agarose microgels are highly suited for *in vitro* experiments which require external treatments or supplementation with antibiotics, growth factors, drugs, lentiviral vectors, and common post-transfection/transformation selection markers. Secondly, the absence of charge interactions negates the possibility of the active agent being sequestered by the biomaterial itself. This enables a precise, reproducible, and tractable experimental design. Furthermore, this functionality of our charge-neutral microgels has significant implications for investigating selection pressures in a

generalized manner in 3D. For instance, substratum stiffness impacts the biofilm formation ability of bacteria [82–87], which may alter drug susceptibility. Phenotypic responses by microbes to variations in surface properties may also be linked to antibiotic resistance mechanisms. From a translational perspective, our experimental setup can help engineer models of complex physiological niches such as tissues. These are often the site of active host-pathogen interactions, wherein selection pressures and adaptive morphologies drastically impact the eventual outcomes.

Agar, agarose, or gelatin have also been extensively employed to encapsulate live bacteria for biomedical applications such as culturing novel microbial strains and efficient *in vivo* delivery of probiotics, as well as to develop high-throughput drug screening platforms [88–93]. In these instances, the microbes are physically constrained within a rigid matrix. We also explore the possibility of encapsulating live GFP-positive *E. coli* cells within the agarose microgel particles. These granules are manufactured using LB broth as both the continuous and dispersed phases. Encapsulated bacteria remain viable and effectively immobilized in 3D space (SI figure 9(B)). Compared to previous attempts, our one-pot synthesis obviates the need for dedicated microfluidic network fabrication, polymeric cross-linking reactions, or extensive washes.

3.5. Embedded 3D bioprinting in jammed agarose microgel media

The ability to spatially arrange cells in 3D with precise control over population shape, size, and composition increase the versatility of a 3D cell growth medium. Further, precisely patterning multiple cells in 3D allows for examining intercellular interactions. While a 3D network of biopolymers (e.g. collagen, matrigel, etc) can support cells in 3D, they do not allow for precise placement of cells in 3D; any insertion of a nozzle through these monolithic matrices creates permanent damage and hence irreversibly alters their mechanical properties. For the same reason, retrieving cells without damaging these monolithic matrices is severely challenging. These challenges are overcome by directly 3D printing cellular constructs inside the jammed microgel systems [26, 28, 29, 34, 38–40, 44, 51–57, 94–104]. 3D bioprinting is a valuable tool for spatially arranging and manipulating cells as per user-defined conformations. We exploit the yield stress nature of jammed agarose microgels to precisely 3D print complex cellular structures inside them. In the presence of a shear force, jammed agarose microgels can transition to a fluid-like material. The shear forces generated by an injection nozzle moving through the jammed microgels in a designated pathway locally fluidize the microgel packing and simultaneously inject cells in the fluidized zone. This fluidized zone reverts to a stable, solid-like conformation once the shear is removed, trapping the cells in the desired location in 3D. The print quality and the surface

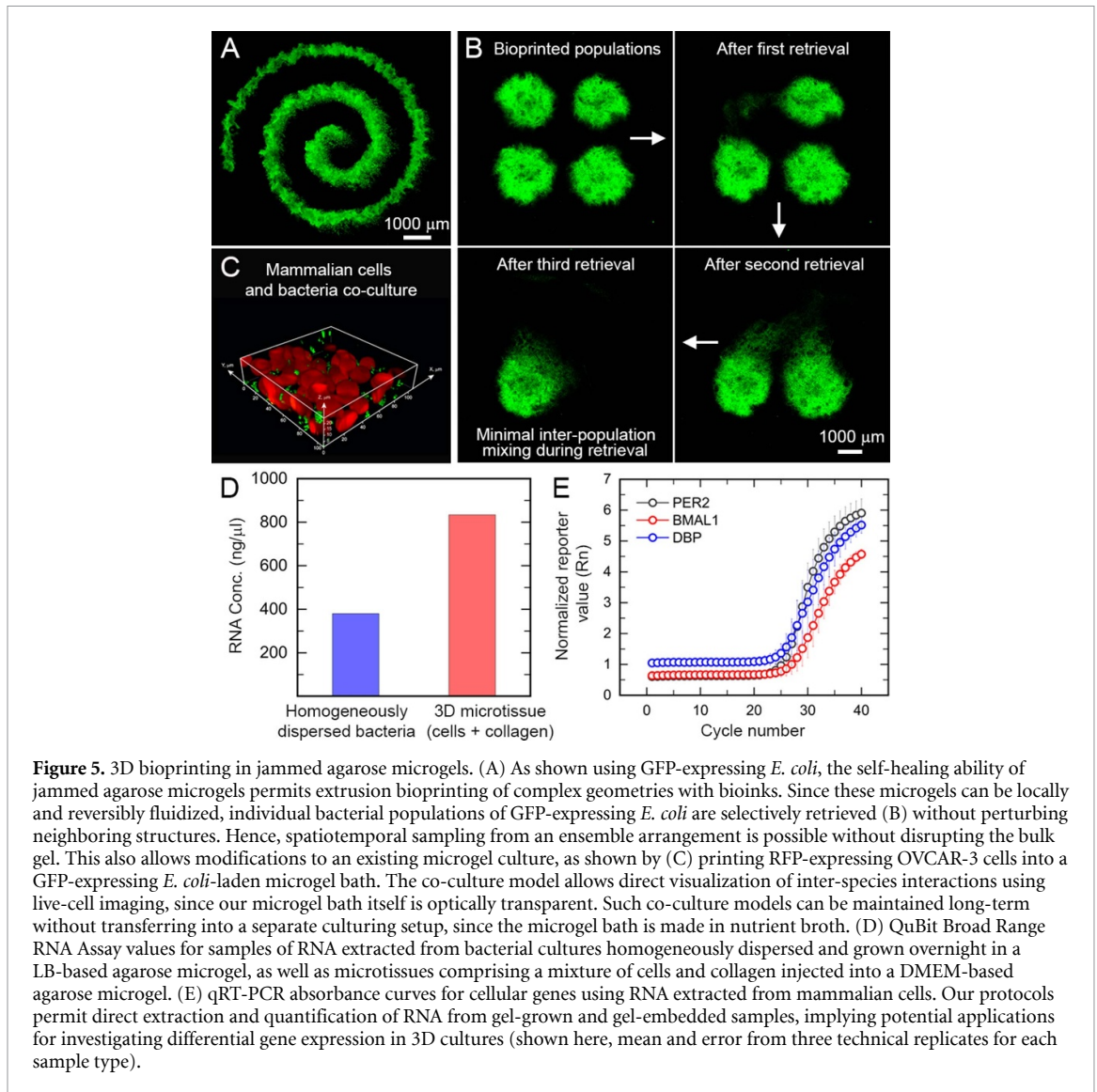


Figure 5. 3D bioprinting in jammed agarose microgels. (A) As shown using GFP-expressing *E. coli*, the self-healing ability of jammed agarose microgels permits extrusion bioprinting of complex geometries with bioinks. Since these microgels can be locally and reversibly fluidized, individual bacterial populations of GFP-expressing *E. coli* are selectively retrieved (B) without perturbing neighboring structures. Hence, spatiotemporal sampling from an ensemble arrangement is possible without disrupting the bulk gel. This also allows modifications to an existing microgel culture, as shown by (C) printing RFP-expressing OVCAR-3 cells into a GFP-expressing *E. coli*-laden microgel bath. The co-culture model allows direct visualization of inter-species interactions using live-cell imaging, since our microgel bath itself is optically transparent. Such co-culture models can be maintained long-term without transferring into a separate culturing setup, since the microgel bath is made in nutrient broth. (D) QuBit Broad Range RNA Assay values for samples of RNA extracted from bacterial cultures homogeneously dispersed and grown overnight in a LB-based agarose microgel, as well as microtissues comprising a mixture of cells and collagen injected into a DMEM-based agarose microgel. (E) qRT-PCR absorbance curves for cellular genes using RNA extracted from mammalian cells. Our protocols permit direct extraction and quantification of RNA from gel-grown and gel-embedded samples, implying potential applications for investigating differential gene expression in 3D cultures (shown here, mean and error from three technical replicates for each sample type).

roughness of 3D printed constructs depend on the granularity of the microgels. Jammed agarose microgels with even smaller granules can be produced by utilizing a tissue homogenizer (SI figure 10). Utilizing this system, we demonstrate the inoculation of bacterial populations of complex geometries inside a 3D growth medium (figure 5(A)).

The potential for the jammed microgel system is not limited to merely 3D bioprinting by patterning bioinks or introducing multiple cell types. Rather, self-healing material property may be exploited to selectively retrieve parts of a printed assemblage with minimal perturbation to other regions. To test this hypothesis, we 3D print four isolated bacterial populations in close vicinity inside agarose microgel media and sequentially retrieve them (figure 5(B)). Even when the inter-population distance is less than their size, we are able to retrieve each population completely without causing any major perturbations. This is a significant advance over cross-linked 3D culturing systems—the rigid, monolithic nature of which render such micro-manipulations untenable. Once

cell populations can be selectively retrieved from the 3D culture, they can be subjected to standard assays such as metabolomics, proteomics, or whole transcriptome sequencing. To prove this concept, we extract RNA from bacterial colonies cultured in jammed agarose microgel growth media, as well as from microtissues composed of mammalian cells seeded in a collagen matrix and suspended within agarose microgels (figure 5(D)). We also carry out qRT-PCR amplification for three different cellular genes using RNA extracted from 3D microtissue samples (figure 5(E)). Together, these two capabilities significantly expand the boundaries of *in vitro* 3D culturing. The selective retrieval strategy combined with RNA extraction and amplification from captured samples allows one to locally and spatiotemporally sample individual niches within a complex system without disrupting the global architecture. This is also true for homogeneous dispersions of cells suspended in the jammed microgels, which may be retrieved and subjected to bulk analysis by the aforementioned methods (SI figure 11). By incorporating micro-scale

mechanical manipulators [105], this could potentially be narrowed down to the single-cell level.

A versatile 3D cell growth medium with the option of 3D bioprinting cellular constructs paves the pathway to a systematic exploration of inter-cellular interactions. Specifically, in the context of infection biology, it has been a longstanding goal to develop physiologically relevant *in vitro* setups to study disease progression. While animal models are vastly superior, they pose challenges to live cell imaging, tissue-level observations in real-time, and standardized control over the experimental dynamics. Co-culture systems using transwells, organoids, and microfluidic setups have tried to address this by incorporating multiple cell types or providing 3D-like culturing conditions, which cannot be realized using conventional monolayer cultures [106]. However, these scaffolds either constrain the interacting populations to an adherent/liquid-suspended state or utilize constrained geometries and flow-based networks, which may disrupt the structural integrity and limit the scale of tissue-like multicellular aggregates. The 3D nature and self-healing ability of agarose microgels help overcome these shortcomings. Briefly, they support cells in a suspended 3D state while allowing temporally separated seeding of distinct cell types within the same system. Additionally, the bath dimensions can be readily adjusted based on the desired culturing scale. Here, we demonstrate a co-culture model of OVCAR-3 cells printed within an *E. coli*-laden RPMI-based jammed agarose microgel bath. Our optically transparent microgel allows real-time imaging of such a system (figure 5(C) and supplementary video). These *in vitro* setups would help model processes such as bacterial or cancer cell invasion of epithelial layers and immune cell dynamics in response to pathogens.

4. Conclusion

Existing microgel-based 3D culturing platforms have vastly expanded our ability to interrogate cellular organization and interactions in settings mimicking physiological niches. These granular systems have been used to arrange, maintain, probe, and manipulate cells in well-defined microenvironments. Furthermore, previous works on porous 3D biomaterials have reported the effect of porosity on cellular morphology, motility, and population-level dynamics [26, 36, 78–81, 107–109]. Combining these hydrogels with 3D bioprinting, an impressive range of structural features has also been rendered. These innovations have served to significantly advance the frontiers of tissue bioengineering and 3D cell culture [26–57, 97–104]. However, in-house fabrication of these microgels involves multi-step synthesis protocols [53, 94, 110], which substantially increases both preparation time and precautions required to maintain sterility. In contrast, many commercially available

microgels [29, 70] are made from negatively charged polyelectrolyte hydrogels that interfere with the bivalent cations of the cell growth media [32]. Additionally, maintaining the sterility of commercially available microgels remains a persistent problem; several microgels are not compatible with either UV or heat sterilization, two of the most widely adopted practices in cell culture laboratories. A 3D medium made of packings of agar/agarose microgels solves this problem. Prior efforts at making agar microgels have used phase separation techniques by introducing either oil or PEG as an emulsifying agent to break up an aqueous solution of molten agarose into discrete particles [111–114]. However, these either involve dedicated microfluidic networks or require extensive wash steps which do not entirely remove traces of the foreign agent. Our approach overcomes these limitations by employing a simple bench-top setup, commonly available mixing equipment, and a one-step synthesis protocol without any additional chemical intermediates or washing steps, which drastically reduces potential chances for contamination. The agarose itself is heat sterilized prior to microgel manufacturing with the additional flexibility for UV sterilization post-manufacture. The ease and simplicity of synthesis put it within reach of most experimental laboratories without any requirement for specialized training or sophisticated equipment. While the flash-solidification strategy presented here substantially increases the throughput, we also recognize the relative merits of existing methods of microparticle manufacturing using microfluidic devices, via droplet generation and emulsification [33, 50, 88, 115–121]. These offer excellent control over particle sizes, geometry, and porosity due to the precisely engineered nature of the synthesis setup. Hence, for specific applications requiring excellent control over individual microparticle and pore space architecture, these remain a superior choice. However, the advantage of our present method is the minimal technical complexity associated with fabrication of micron-sized granules, which can be achieved without sophisticated equipment and within extremely short experimental times.

Jammed agarose microgels provide an extremely dynamic 3D platform that can simultaneously host diverse cell types and inter-species co-cultures, enable high-quality live cell imaging, be functionally compatible with commonly used selection markers, allow 3D bioprinting with live bioinks, and permit localized sampling. Our study hence lays the groundwork for a highly accessible and versatile 3D culturing platform. Both the modular synthesis process and the inert nature of agarose contribute to the versatility. The non-reactive property is important for live-cell encapsulation without affecting the surface properties of the cells, since agarose does not carry residual charges. The charge neutrality of this polymer also allows antibiotics-based selection, unlike many

existing 3D platforms which use charged microgel particles. The distinct advantages in terms of chemical inertness and charge neutrality greatly expand its applicability for high-throughput screening applications. It is also possible to incorporate selective experimental cues—for instance, pharmacological agents and growth/differentiation factors—while following existing protocols designed for conventional 2D systems.

Jammed microgels also serve as scaffolds to assemble complex, multicellular, tissue-mimicking structures. This is made possible by extrusion bioprinting, which confers the ability to spatially arrange cells in 3D. Designing tissue-like mimics is feasible using our scaffold since the bulk gel can be modified to make it suitable for adherent cell culture. In a significant advance over several existing rigid 3D scaffolds, we can spatiotemporally probe and retrieve samples without perturbing or compromising the structural integrity of the system. This feature, in combination with our capability to extract RNA from agarose microgel samples, suggests possibilities to study differential gene expression in 3D cell culture models. With further optimizations, this could likely be extended to cover the transcriptome, proteome, and metabolome domains as well. Hence, we envision extremely promising avenues for further advances in 3D cell culture, bioprinting, and tissue bioengineering using jammed agarose microgels. Promising future directions include culturing organoids, stem cells, T-cells, and patient-derived primary cell cultures in this matrix. We hypothesize that difficult-to-culture cell types—such as those obtained from *ex vivo* explants—may be cultured by both stiffness matching agarose microgels to their physiological organ/tissue origins, as well as incorporating ECM components within the 3D growth media, which would allow researchers to reproducibly mimic key aspects of their *in vivo* microenvironments in a controlled manner.

The disordered, porous, and granular architecture of jammed agarose microgels mimics scenarios frequently encountered by soil and gut mucus-resident bacteria, which navigate porous environments that are structurally similar to polymeric microgels. Current efforts towards understanding microbial evolution under various external cues and selection pressures typically employ flat-plate or liquid cultures over several passages. The jammed microgel platform presented here offers an unprecedented opportunity to expand the scope of such studies by integrating tunable mechanics and antibiotic treatment within a granular, porous media—thereby enabling a more effective and controlled *in vitro* modeling of diverse physiological niches. This charge-neutral matrix also opens up future opportunities to study electrotaxis in 3D. Furthermore, since the shear moduli of individual agarose granules is of the order of ~ 10 kPa, they can withstand shear forces due

to fluid flow. Thus, the solid packings of agarose granules can be easily housed in confined chambers, and leveraging the transparent nature of fluid flow through the inter-microgel pores can be easily visualized. Hence, the jammed agarose microgels can be used to study bacterial migration through a porous medium under flow and the transition of planktonic cells to form biofilms under local confinement. Similarly, by flowing nutrient-rich medium bioprinted cellular constructs can be maintained for long-term inside jammed microgel growth media. Finally, we envision that by flowing selective morphogens through the jammed agarose microgels, 3D bioprinted constructs can be differentiated to create multi-functional organoids.

Data availability statement

All data that support the findings of this study are included within the article (and any supplementary files).

Acknowledgments


We acknowledge Professor Robert Austin for providing us with the *E. coli* cells, Dr Shashi Thutupalli for giving us the yeast cells, and Dr Shaon Chakrabarti for providing 3T3 H2B BFP cells, as well as qRT-PCR protocols and reagents. We thank Dr Sudarshan Gadadhar for providing 3T3 GFP cells. We are grateful to Dr H Krishnamurthy and the Central Imaging and Flow Cytometry Facility at NCBS. We also acknowledge the NCBS common equipment facility for arranging the Anton Parr MCR 302e rheometer and NextGen sequencing facility for arranging Qubit. We thank Ashitha B Arun, Jimpi Langthasa, Shyamili Goutham, and Mallar Banerjee for sharing cell culture protocols as well as for assistance with the experiments. T B acknowledges intramural research grant from NCBS. M S acknowledges personal support through NCBS GS program. R B acknowledges support from the Wellcome Trust/DBT India Alliance (IA/I/17/2/503312) and the Department of Biotechnology, India (DBT) (BT/909 PR26526/GET/119/92/2017).

Author contributions

T B designed and conceptualized the overall project. R B provided essential guidance and support for cell viability studies. M S, with critical help from M G, performed all the experiments and analyzed data. All authors participated in writing the manuscript.

ORCID iDs

M Sreepadmanabh  <https://orcid.org/0000-0003-3492-0203>

Ramray Bhat  <https://orcid.org/0000-0002-5215-9721>

Tapomoy Bhattacharjee  <https://orcid.org/0000-0001-8899-1379>

References

- [1] Baker B M and Chen C S 2012 Deconstructing the third dimension: how 3D culture microenvironments alter cellular cues *J. Cell Sci.* **125** 3015–24
- [2] Petersen O W, Rønnov-Jessen L, Howlett A R and Bissell M J 1992 Interaction with basement membrane serves to rapidly distinguish growth and differentiation pattern of normal and malignant human breast epithelial cells *Proc. Natl Acad. Sci. USA* **89** 9064–8
- [3] Benya P D and Shaffer J D 1982 Dedifferentiated chondrocytes reexpress the differentiated collagen phenotype when cultured in agarose gels *Cell* **30** 215–24
- [4] Lee E Y, Parry G and Bissell M J 1984 Modulation of secreted proteins of mouse mammary epithelial cells by the collagenous substrata *J. Cell Biol.* **98** 146–55
- [5] Luca A C et al 2013 Impact of the 3D microenvironment on phenotype, gene expression, and EGFR inhibition of colorectal cancer cell lines *PLoS One* **8** e59689
- [6] Velez D O, Ranamukhaarachchi S K, Kumar A, Modi R N, Lim E W, Engler A J, Metallo C M and Fraley S I 2019 3D collagen architecture regulates cell adhesion through degradability, thereby controlling metabolic and oxidative stress *Integr. Biol.* **11** 221–34
- [7] Mekala N K, Baadhe R R and Potumarthi R 2014 Mass transfer aspects of 3D cell cultures in tissue engineering *Asia-Pac. J. Chem. Eng.*, **9** 318–29
- [8] Lagies S, Schlimpert M, Neumann S, Wäldin A, Kammerer B, Borner C and Peintner L 2020 Cells grown in three-dimensional spheroids mirror *in vivo* metabolic response of epithelial cells *Commun. Biol.* **3** 246
- [9] Kusuma G D et al 2022 Effect of 2D and 3D culture microenvironments on mesenchymal stem cell-derived extracellular vesicles potencies *Front. Cell Dev. Biol.* **10** 819726
- [10] Duval K, Grover H, Han L-H, Mou Y, Pegoraro A F, Fredberg J and Chen Z 2017 Modeling physiological events in 2D vs. 3D cell culture *Physiology* **32** 266–77
- [11] Song A S, Najjar A M and Diller K R 2014 Thermally induced apoptosis, necrosis, and heat shock protein expression in 3D culture *J. Biomech. Eng.* **136** 071006
- [12] Rocha S et al 2019 3D cellular architecture affects MicroRNA and protein cargo of extracellular vesicles *Adv. Sci.* **6** 1800948
- [13] Anada T, Fukuda J, Sai Y and Suzuki O 2012 An oxygen-permeable spheroid culture system for the prevention of central hypoxia and necrosis of spheroids *Biomaterials* **33** 8430–41
- [14] Luo L et al 2021 A novel 3D culture model of human ASCs reduces cell death in spheroid cores and maintains inner cell proliferation compared with a nonadherent 3D culture *Front. Cell Dev. Biol.* **9** 737275
- [15] Martinez-Calvo A, Bhattacharjee T, Bay R K, Luu H N, Hancock A M, Wingreen N S and Datta S S 2022 Morphological instability and roughening of growing 3D bacterial colonies *Proc. Natl Acad. Sci. USA* **119** e2208019119
- [16] Mammoto A, Mammoto T and Ingber D E 2012 Mechanosensitive mechanisms in transcriptional regulation *J. Cell Sci.* **125** 3061–73
- [17] Pelham R J Jr and Wang Y 1997 Cell locomotion and focal adhesions are regulated by substrate flexibility *Proc. Natl Acad. Sci. USA* **94** 13661–5
- [18] Cukierman E, Pankov R, Stevens D R and Yamada K M 2001 Taking cell-matrix adhesions to the third dimension *Science* **294** 1708–12
- [19] Discher D E, Janmey P and Wang Y L 2005 Tissue cells feel and respond to the stiffness of their substrate *Science* **310** 1139–43
- [20] Fraley S I, Feng Y, Krishnamurthy R, Kim D-H, Celedon A, Longmore G D and Wirtz D 2010 A distinctive role for focal adhesion proteins in three-dimensional cell motility *Nat. Cell Biol.* **12** 598–604
- [21] Chaudhuri O, Cooper-White J, Janmey P A, Mooney D J and Shenoy V B 2020 Effects of extracellular matrix viscoelasticity on cellular behaviour *Nature* **584** 535–46
- [22] Wei S C et al 2015 Matrix stiffness drives epithelial-mesenchymal transition and tumour metastasis through a TWIST1-G3BP2 mechanotransduction pathway *Nat. Cell Biol.* **17** 678–88
- [23] Engler A J, Sen S, Sweeney H L and Discher D E 2006 Matrix elasticity directs stem cell lineage specification *Cell* **126** 677–89
- [24] Evans N D, Minelli C, Gentleman E, LaPointe V, Patankar S N, Kallivretaki M, Chen X, Roberts C J and Stevens M M 2009 Substrate stiffness affects early differentiation events in embryonic stem cells *Eur. Cell Mater.* **18** 1–13
- [25] Ravi M, Paramesh V, Kaviya S R, Anuradha E and Solomon F D P 2015 3D cell culture systems: advantages and applications *J. Cell. Physiol.* **230** 16–26
- [26] Bhattacharjee T et al 2016 Liquid-like solids support cells in 3D *ACS Biomater. Sci. Eng.* **2** 1787–95
- [27] Akther F, Little P, Li Z, Nguyen N-T and Ta H T 2020 Hydrogels as artificial matrices for cell seeding in microfluidic devices *RSC Adv.* **10** 43682–703
- [28] Lee A, Hudson A R, ShiwarSKI D J, Tashman J W, Hinton T J, Yerneni S, Bliley J M, Campbell P G and Feinberg A W 2019 3D bioprinting of collagen to rebuild components of the human heart *Science* **365** 482–7
- [29] O'Bryan C S, Bhattacharjee T, Marshall S L, Gregory Sawyer W and Angelini T E 2018 Commercially available microgels for 3D bioprinting *Bioprinting* **11** e00037
- [30] Deforest C A, Sims E A and Anseth K S 2010 Peptide-functionalized click hydrogels with independently tunable mechanics and chemical functionality for 3D cell culture *Chem. Mater.* **22** 4783–90
- [31] Morley C D, Tordoff J, O'Bryan C S, Weiss R and Angelini T E 2020 3D aggregation of cells in packed microgel media *Soft Matter* **16** 6572–81
- [32] O'Bryan C S, Kabb C P, Sumerlin B S and Angelini T E 2019 Jammed polyelectrolyte microgels for 3D cell culture applications: rheological behavior with added salts *ACS Appl. Bio Mater.* **2** 1509–17
- [33] Mohamed M G A, Ambhorkar P, Samanipour R, Yang A, Ghafoor A and Kim K 2020 Microfluidics-based fabrication of cell-laden microgels *Biomicrofluidics* **14** 021501
- [34] Feng Q, Li D, Li Q, Li H, Wang Z, Zhu S, Lin Z, Cao X and Dong H 2022 Assembling microgels via dynamic cross-linking reaction improves printability, microporosity, tissue-adhesion, and self-healing of microgel bioink for extrusion bioprinting *ACS Appl. Mater. Interfaces* **14** 15653–66
- [35] Molley T G, Hung T T and Kilian K A 2022 Cell-laden gradient microgel suspensions for spatial control of differentiation during biofabrication *Adv. Healthcare Mater.* **11** 2201122
- [36] Bhattacharjee T and Angelini T E 2018 3D T cell motility in jammed microgels *J. Phys. D: Appl. Phys.* **52** 024006
- [37] Caliani S R and Burdick J A 2016 A practical guide to hydrogels for cell culture *Nat. Methods* **13** 405–14
- [38] Song K, Compaan A M, Chai W and Huang Y 2020 Injectable gelatin microgel-based composite ink for 3D bioprinting in air *ACS Appl. Mater. Interfaces* **12** 22453–66
- [39] Song K, Zhang D, Yin J and Huang Y 2021 Computational study of extrusion bioprinting with jammed gelatin microgel-based composite ink *Addit. Manuf.* **41** 101963
- [40] Moon D, Lee M-G, Sun J-Y, Song K H and Doh J 2022 Jammed microgel-based inks for 3D printing of complex

- structures transformable via pH/temperature variations *Macromol. Rapid Commun.* **43** 2200271
- [41] Griffin D R, Weaver W M, Scumpia P O, Di Carlo D and Segura T 2015 Accelerated wound healing by injectable microporous gel scaffolds assembled from annealed building blocks *Nat. Mater.* **14** 737–44
- [42] Sideris E, Griffin D R, Ding Y, Li S, Weaver W M, Di Carlo D, Hsiai T and Segura T 2016 Particle hydrogels based on hyaluronic acid building blocks *ACS Biomater. Sci. Eng.* **2** 2034–41
- [43] Phelps E A, Enemchukwu N O, Fiore V F, Sy J C, Murthy N, Sulchek T A, Barker T H and Garcia A J 2012 Maleimide cross-linked bioactive PEG hydrogel exhibits improved reaction kinetics and cross-linking for cell encapsulation and *in situ* delivery *Adv. Mater.* **24** 64–70
- [44] Jeon O, Lee Y B, Hinton T J, Feinberg A W and Alsberg E 2019 Cryopreserved cell-laden alginate microgel bioink for 3D bioprinting of living tissues *Mater. Today Chem.* **12** 61–70
- [45] Sheikhi A, de Rutte J, Haghniaz R, Akouissi O, Sohrabi A, Di Carlo D and Khademhosseini A 2019 Microfluidic-enabled bottom-up hydrogels from annealable naturally-derived protein microbeads *Biomaterials* **192** 560–8
- [46] Kim P-H, Yim H-G, Choi Y-J, Kang B-J, Kim J, Kwon S-M, Kim B-S, Hwang N S and Cho J-Y 2014 Injectable multifunctional microgel encapsulating outgrowth endothelial cells and growth factors for enhanced neovascularization *J. Control. Release* **187** 1–13
- [47] Qazi T H and Burdick J A 2021 Granular hydrogels for endogenous tissue repair *Biomater. Biosyst.* **1** 100008
- [48] Caldwell A S et al 2017 Clickable microgel scaffolds as platforms for 3D cell encapsulation *Adv. Healthcare Mater.* **6** 15
- [49] Rommel D, Mork M, Vedaraman S, Bastard C, Guerzoni L P B, Kittel Y, Vinokur R, Born N, Haraszti T and De Laporte L 2022 Functionalized microgel rods interlinked into soft macroporous structures for 3D cell culture *Adv. Sci.* **9** e2103554
- [50] Yang C-H, Lin Y-S, Huang K-S, Huang Y-C, Wang E-C, Jhong J-Y and Kuo C-Y 2009 Microfluidic emulsification and sorting assisted preparation of monodisperse chitosan microparticles *Lab Chip* **9** 145–50
- [51] Bhattacharjee T, Zehnder S M, Rowe K G, Jain S, Nixon R M, Sawyer W G and Angelini T E 2015 Writing in the granular gel medium *Sci. Adv.* **1** e1500655
- [52] Highley C B, Rodell C B and Burdick J A 2015 Direct 3D printing of shear-thinning hydrogels into self-healing hydrogels *Adv. Mater.* **27** 5075–9
- [53] Hinton T J, Jallerat Q, Palchesko R N, Park J H, Grodzicki M S, Shue H-J, Ramadan M H, Hudson A R and Feinberg A W 2015 Three-dimensional printing of complex biological structures by freeform reversible embedding of suspended hydrogels *Sci. Adv.* **1** e1500758
- [54] Ouyang L, Highley C B, Rodell C B, Sun W and Burdick J A 2016 3D printing of shear-thinning hyaluronic acid hydrogels with secondary cross-linking *ACS Biomater. Sci. Eng.* **2** 1743–51
- [55] O'Bryan C S, Bhattacharjee T, Niemi S R, Balachandrar S, Baldwin N, Ellison S T, Taylor C R, Sawyer W G and Angelini T E 2017 Three-dimensional printing with sacrificial materials for soft matter manufacturing *MRS Bull.* **42** 571–7
- [56] O'Bryan C S, Bhattacharjee T, Hart S, Kabb C P, Schulze K D, Chilakala I, Sumerlin B S, Sawyer W G and Angelini T E 2017 Self-assembled micro-organogels for 3D printing silicone structures *Sci. Adv.* **3** e1602800
- [57] Highley C B, Song K H, Daly A C and Burdick J A 2019 Jammed microgel inks for 3D printing applications *Adv. Sci.* **6** 1801076
- [58] Langthasa J, Sarkar P, Narayanan S, Bhagat R, Vadaparty A and Bhat R 2021 Extracellular matrix mediates moruloid-blastuloid morphodynamics in malignant ovarian spheroids *Life Sci. Alliance* **4** e20200942
- [59] Sung K, Khan S A, Nawaz M S and Khan A A 2003 A simple and efficient triton X-100 boiling and chloroform extraction method of RNA isolation from gram-positive and gram-negative bacteria *FEMS Microbiol. Lett.* **229** 97–101
- [60] Lee P Y, Costumbrado J, Hsu C-Y and Kim Y H 2012 Agarose gel electrophoresis for the separation of DNA fragments *J. Vis. Exp.* **62** 3923
- [61] Renn D W 1984 Agar and agarose: indispensable partners in biotechnology *Ind. Eng. Chem. Product Res. Dev.* **23** 17–21
- [62] Li M, Fu T, Yang S, Pan L, Tang J, Chen M, Liang P, Gao Z and Guo L 2021 Agarose-based spheroid culture enhanced stemness and promoted odontogenic differentiation potential of human dental follicle cells *in vitro* *Vitro Cell. Dev. Biol.* **57** 620–30
- [63] Gao W, Wu D, Wang Y, Wang Z, Zou C, Dai Y, Ng C-F, Teoh J Y-C and Chan F L 2018 Development of a novel and economical agar-based non-adherent three-dimensional culture method for enrichment of cancer stem-like cells *Stem Cell Res. Ther.* **9** 243
- [64] Reis R L et al 2008 *Natural-Based Polymers for Biomedical Applications* (Cambridge: Elsevier Ltd) pp 1–802
- [65] Ichinose N and Ura H 2020 Concentration dependence of the sol-gel phase behavior of agarose-water system observed by the optical bubble pressure tensiometry *Sci. Rep.* **10** 1–9
- [66] Subhash G, Liu Q, Moore D F, Ifju P G and Haile M A 2010 Concentration dependence of tensile behavior in agarose gel using digital image correlation *Exp. Mech.* **51** 255–62
- [67] Narayanan J, Xiong J Y and Liu X Y 2006 Determination of agarose gel pore size: absorbance measurements vis a vis other techniques *J. Phys.: Conf. Ser.* **28** 83
- [68] Zarrintaj P, Manouchehri S, Ahmadi Z, Saeb M R, Urbanska A M, Kaplan D L and Mozafari M 2018 Agarose-based biomaterials for tissue engineering *Carbohydrate Polym.* **187** 66–84
- [69] Lefroy K S, Murray B S and Ries M E 2021 Advances in the use of microgels as emulsion stabilisers and as a strategy for cellulose functionalisation *Cellulose* **28** 647–70
- [70] Bhattacharjee T, Kabb C P, O'Bryan C S, Uruña J M, Sumerlin B S, Sawyer W G and Angelini T E 2018 Polyelectrolyte scaling laws for microgel yielding near jamming *Soft Matter* **14** 1559–70
- [71] van Oosten A S G, Chen X, Chin L, Cruz K, Patteson A E, Pogoda K, Shenoy V B and Janmey P A 2019 Emergence of tissue-like mechanics from fibrous networks confined by close-packed cells *Nature* **573** 96–101
- [72] Benton J A, DeForest C A, Vivekanandan V and Anseth K S 2009 Photocrosslinking of gelatin macromers to synthesize porous hydrogels that promote valvular interstitial cell function *Tissue Eng. A* **15** 3221–30
- [73] DeForest C A and Anseth K S 2011 Cytocompatible click-based hydrogels with dynamically tunable properties through orthogonal photoconjugation and photocleavage reactions *Nat. Chem.* **3** 925–31
- [74] DeForest C A, Polizzotti B D and Anseth K S 2009 Sequential click reactions for synthesizing and patterning three-dimensional cell microenvironments *Nat. Mater.* **8** 659–64
- [75] DeForest C A and Tirrell D A 2015 A photoreversible protein-patterning approach for guiding stem cell fate in three-dimensional gels *Nat. Mater.* **14** 523–31
- [76] Ruskowitz E R and DeForest C A 2018 Photoresponsive biomaterials for targeted drug delivery and 4D cell culture *Nat. Rev. Mater.* **3** 1–17
- [77] Shadish J A, Benuska G M and DeForest C A 2019 Bioactive site-specifically modified proteins for 4D patterning of gel biomaterials *Nat. Mater.* **18** 1005–14

- [78] Bhattacharjee T, Amchin D B, Alert R, Ott J A and Datta S S 2022 Chemotactic smoothing of collective migration *eLife* **11** e71226
- [79] Bhattacharjee T, Amchin D B, Ott J A, Kratz F and Datta S S 2021 Chemotactic migration of bacteria in porous media *Biophys. J.* **120** 3483–97
- [80] Bhattacharjee T and Datta S S 2019 Confinement and activity regulate bacterial motion in porous media *Soft Matter* **15** 9920–30
- [81] Bhattacharjee T and Datta S S 2019 Bacterial hopping and trapping in porous media *Nat. Commun.* **10** 1–9
- [82] Asp M E, Ho Thanh M-T, Germann D A, Carroll R J, Franceschi A, Welch R D, Gopinath A and Pattenon A E 2022 Spreading rates of bacterial colonies depend on substrate stiffness and permeability *PNAS Nexus* **1** 1–13
- [83] Bottura B, Rooney L M, Hoskisson P A and McConnell G 2022 Intra-colony channel morphology in *Escherichia coli* biofilms is governed by nutrient availability and substrate stiffness *Biofilm* **4** 100084
- [84] Epstein A K, Hochbaum A I, Kim P and Aizenberg J 2011 Control of bacterial biofilm growth on surfaces by nanostructural mechanics and geometry *Nanotechnology* **22** 494007
- [85] Gomez S *et al* 2023 Substrate stiffness impacts early biofilm formation by modulating *Pseudomonas aeruginosa* twitching motility *eLife* **12** e81112
- [86] Song F 2016 Effects of substrate stiffness on bacterial biofilm formation *Dissertations* (available at: <https://surface.syr.edu/etd/453>)
- [87] Zheng S, Bawazir M, Dhall A, Kim H-E, He L, Heo J and Hwang G 2021 Implication of surface properties, bacterial motility, and hydrodynamic conditions on bacterial surface sensing and their initial adhesion *Front. Bioeng. Biotechnol.* **9** 82
- [88] Eun Y J, Utada A S, Copeland M F, Takeuchi S and Weibel D B 2011 Encapsulating bacteria in agarose microparticles using microfluidics for high-throughput cell analysis and isolation *ACS Chem. Biol.* **6** 260
- [89] Ben-Dov E, Kramarsky-Winter E and Kushmaro A 2009 An *in situ* method for cultivating microorganisms using a double encapsulation technique *FEMS Microbiol. Ecol.* **68** 363–71
- [90] Pour H M, Marhamatizadeh M H and Fattahi H 2022 Encapsulation of different types of probiotic bacteria within conventional/multilayer emulsion and its effect on the properties of probiotic yogurt *J. Food Qual.* **2022** 1–12
- [91] Pupa P *et al* 2021 The efficacy of three double-microencapsulation methods for preservation of probiotic bacteria *Sci. Rep.* **11** 1–9
- [92] Li X Y *et al* 2009 Microencapsulation of a probiotic bacteria with alginate–gelatin and its properties *J. Microencapsul.* **26** 315–24
- [93] Albadran H A, Monteagudo-Mera A, Khutoryanskiy V V and Charalampopoulos D 2020 Development of chitosan-coated agar-gelatin particles for probiotic delivery and targeted release in the gastrointestinal tract *Appl. Microbiol. Biotechnol.* **104** 5749–57
- [94] Hinton T J, Hudson A, Pusch K, Lee A and Feinberg A W 2016 3D printing PDMS elastomer in a hydrophilic support bath via freeform reversible embedding *ACS Biomater. Sci. Eng.* **2** 1781–6
- [95] Morley C D *et al* 2019 Quantitative characterization of 3D bioprinted structural elements under cell generated forces *Nat. Commun.* **10** 1–9
- [96] Zhang Y, Ellison S T, Duraivel S, Morley C D, Taylor C R and Angelini T E 2021 3D printed collagen structures at low concentrations supported by jammed microgels *Bioprinting* **21** e00121
- [97] Mendes B B, Daly A C, Reis R L, Domingues R M A, Gomes M E and Burdick J A 2021 Injectable hyaluronic acid and platelet lysate-derived granular hydrogels for biomedical applications *Acta Biomater.* **119** 101–13
- [98] Seymour A J, Shin S and Heilshorn S C 2021 3D printing of microgel scaffolds with tunable void fraction to promote cell infiltration *Adv. Healthcare Mater.* **10** 2100644
- [99] Patrício S G, Sousa L R, Correia T R, Gaspar V M, Pires L S, Luís J L, Oliveira J M and Mano J F 2020 Freeform 3D printing using a continuous viscoelastic supporting matrix *Biofabrication* **12** 035017
- [100] Xin S *et al* 2013 Clickable PEG hydrogel microspheres as building blocks for 3D bioprinting *Biomater. Sci.* **7** 1–3
- [101] Xin S, Deo K A, Dai J, Pandian N K R, Chimene D, Moebius R M, Jain A, Han A, Gaharwar A K and Alge D L 2021 Generalizing hydrogel microparticles into a new class of bioinks for extrusion bioprinting *Sci. Adv.* **7** eabk3087
- [102] Molley T G, Jalandhra G K, Nemeč S R, Tiffany A S, Patkunarajah A, Poole K, Harley B A C, Hung T-T and Kilian K A 2021 Heterotypic tumor models through freeform printing into photostabilized granular microgels *Biomater. Sci.* **9** 4496–509
- [103] Chen Z, Zhao D, Liu B, Nian G, Li X, Yin J, Qu S and Yang W 2019 3D printing of multifunctional hydrogels *Adv. Funct. Mater.* **29** 1900971
- [104] Fang Y, Guo Y, Ji M, Li B, Guo Y, Zhu J, Zhang T and Xiong Z 2022 3D printing of cell-laden microgel-based biphasic bioink with heterogeneous microenvironment for biomedical applications *Adv. Funct. Mater.* **32** 2109810
- [105] Ellison S T, Duraivel S, Subramaniam V, Hugosson F, Yu B, Lebowitz J J, Khoshbouei H, Lele T P, Martindale M Q and Angelini T E 2022 Cellular micromasonry: biofabrication with single cell precision *Soft Matter* **18** 8554–60
- [106] Sreepadmanabh M and Toley B J 2018 Investigations into the cancer stem cell niche using *in-vitro* 3D tumor models and microfluidics *Biotechnol. Adv.* **36** 1094–110
- [107] Santos H A 2012 Porous-based biomaterials for tissue engineering and drug delivery applications *Biomater* **2** 237–8
- [108] Hernandez J L and Woodrow K A 2022 Medical applications of porous biomaterials: features of porosity and tissue-specific implications for biocompatibility *Adv. Healthcare Mater.* **11** e2102087
- [109] Maksoud F J, Velázquez de la Paz M F, Hann A J, Thanarak J, Reilly G C, Claeysens F, Green N H and Zhang Y S 2022 Porous biomaterials for tissue engineering: a review *J. Mater. Chem. B* **10** 8111–65
- [110] Muir V G, Prendergast M E and Burdick J A 2022 Fragmenting bulk hydrogels and processing into granular hydrogels for biomedical applications *J. Vis. Exp.* **2022** 183
- [111] Kuroiwa T, Katsumata T, Sukeda Y, Warashina S, Kobayashi I, Uemura K and Kanazawa A 2016 Formulation of uniform-sized agar gel microbeads from water-in-oil emulsion prepared using microchannel emulsification under controlled temperature *Japan J. Food Eng.* **17** 11–19
- [112] Zhou Q Z, Wang L-Y, Ma G-H and Su Z-G 2007 Preparation of uniform-sized agarose beads by microporous membrane emulsification technique *J. Colloid Interface Sci.* **311** 118–27
- [113] Li C and Liu C 2018 Characterization of agarose microparticles prepared by water-in-water emulsification *Part. Sci. Technol.* **36** 592–9
- [114] Mu Y, Lyddiatt A and Pacey A W 2005 Manufacture by water/oil emulsification of porous agarose beads: effect of processing conditions on mean particle size, size distribution and mechanical properties *Chem. Eng. Process.* **44** 1157–66
- [115] Hwang D K, Dendukuri D and Doyle P S 2008 Microfluidic-based synthesis of non-spherical magnetic hydrogel microparticles *Lab Chip* **8** 1640–7
- [116] Duncanson W J, Lin T, Abate A R, Seiffert S, Shah R K and Weitz D A 2012 Microfluidic synthesis of advanced microparticles for encapsulation and controlled release *Lab Chip* **12** 2135–45

- [117] Kim D-Y, Jin S H, Jeong S-G, Lee B, Kang K-K and Lee C-S 2018 Microfluidic preparation of monodisperse polymeric microspheres coated with silica nanoparticles *Sci. Rep.* **8** 8525
- [118] Li W *et al* 2018 Microfluidic fabrication of microparticles for biomedical applications *Chem. Soc. Rev.* **47** 5646–83
- [119] Shi Z, Lai X, Sun C, Zhang X, Zhang L, Pu Z, Wang R, Yu H and Li D 2020 Step emulsification in microfluidic droplet generation: mechanisms and structures *Chem. Commun.* **56** 9056–66
- [120] Chung C H Y, Lau C M L, Sin D T, Chung J T, Zhang Y, Chau Y and Yao S 2021 Droplet-based microfluidic synthesis of hydrogel microparticles via click chemistry-based cross-linking for the controlled release of proteins *ACS Appl. Bio Mater.* **4** 6186–94
- [121] Galvan-Chacon V P, Costa L, Barata D and Habibovic P 2021 Droplet microfluidics as a tool for production of bioactive calcium phosphate microparticles with controllable physicochemical properties *Acta Biomater.* **128** 486–501